Cell, Vol. 98, 487–499, August 20, 1999, Copyright ©1999 by Cell Press

Store-Operated Ca^{2+} Entry: Evidence for a Secretion-like Coupling Model

Randen L. Patterson, Damian B. van Rossum, and Donald L. Gill*
Department of Biochemistry and Molecular Biology
University of Maryland School of Medicine
Baltimore, Maryland 21201

Summary

The elusive coupling between endoplasmic reticulum (ER) Ca^{2+} stores and plasma membrane (PM) "store-operated" Ca^{2+} entry channels was probed through a novel combination of cytoskeletal modifications. Whereas coupling was unaffected by disassembly of the actin cytoskeleton, in situ redistribution of F-actin into a tight cortical layer subjacent to the PM displaced cortical ER and prevented coupling between ER and PM Ca^{2+} entry channels, while not affecting inositol 1,4,5-trisphosphate-mediated store release. Importantly, disassembly of the induced cortical actin layer allowed ER to regain access to the PM and reestablish coupling of Ca^{2+} entry channels to Ca^{2+} store depletion. Coupling is concluded to be mediated by a physical "secretion-like" mechanism involving close but reversible interactions between the ER and the PM.

Introduction

Ca^{2+} signals control a vast array of cellular functions ranging from short-term responses such as contraction and secretion to longer-term regulation of cell growth and proliferation (Berridge et al., 1998). The generation of receptor-induced cytosolic Ca^{2+} signals involves two interdependent and closely coupled components: rapid, transient release of Ca^{2+} stored in the endoplasmic reticulum (ER), followed by slowly developing extracellular Ca^{2+} entry (Putney and Bird, 1993; Parekh and Penner, 1997; Berridge et al., 1998; Putney and McKay, 1999). Phospholipase C–coupled receptors generate the chemical messenger, inositol 1,4,5-trisphosphate ($InsP_3$), that diffuses rapidly from the plasma membrane (PM) to interact with $InsP_3$ receptors on the ER that serve as Ca^{2+} channels to release luminal Ca^{2+} and generate the initial Ca^{2+} signal phase (Berridge et al., 1998). The resulting depletion of ER Ca^{2+} serves as the trigger for a message that is returned to the PM, resulting in slow activation of "store-operated channels" (SOCs) mediating Ca^{2+} entry (Putney and Bird, 1993; Gill et al., 1996; Parekh and Penner, 1997; Putney and McKay, 1999). This second phase of Ca^{2+} signals mediates longer-term cytosolic Ca^{2+} elevations and replenishes intracellular stores (Putney and Bird, 1993; Parekh and Penner, 1997).

Whereas generation of $InsP_3$ and activation of Ca^{2+} release channels mediating the initial Ca^{2+} signaling phase are well understood, the mechanism for coupling ER Ca^{2+} store depletion with Ca^{2+} entry remains a crucial question (Putney and McKay, 1999). Evidence for a chemical messenger released from ER has been reported (Randriamanpita and Tsien, 1993; Csutora et al., 1999), but no messenger molecule has been identified. Alternatively, a direct coupling mechanism involving physical interaction between ER and PM was proposed by Irvine (1990) and Berridge (1995), and a possible role of the $InsP_3$ receptor in such coupling has been provided by Kiselyov et al. (1998). Consistent with a direct coupling mechanism are studies indicating $InsP_3$-induced Ca^{2+} store emptying is localized in regions close to Ca^{2+} entry sites (Petersen and Berridge, 1996; Parekh and Penner, 1997). However, one implication of direct coupling would be the expectation of rapid SOC activation. Rather, SOC activation is slow, requiring tens to hundreds of seconds to develop (Hoth and Penner, 1993; Zweifach and Lewis, 1993; Parekh and Penner, 1997; Kerschbaum and Cahalan, 1999). Moreover, considering the rapidity of $InsP_3$-mediated store emptying, the slow activation of Ca^{2+} entry is inconsistent with a messenger molecule released from the ER and traveling the same distance as $InsP_3$ to activate SOCs in the PM.

We therefore considered a coupling mechanism that combines probable close interaction between ER and the PM but is more consistent with the protracted kinetics of SOC activation. Physical trafficking of ER toward the PM was a plausible model, and, indeed, such a mechanism has been considered (Putney and Bird, 1993; Parekh and Penner, 1997). In support of this, small GTP-binding proteins modulate trafficking and are strongly implicated in SOC coupling (Bird and Putney, 1993; Fasolato et al., 1993; Somasundaram et al., 1995; Fernando et al., 1997; Parekh and Penner, 1997). Moreover, $InsP_3$ receptor-rich ER membranes undergo a reversible coupling process requiring GTP that activates Ca^{2+} movement across unidentified target membranes (Gill et al., 1993, 1996; Rys-Sikora et al., 1994; Rys-Sikora and Gill, 1998). A trafficking model for SOC activation has obvious parallels with the secretory pathway and predicts that cytoskeletal elements close to the PM could exert a modifying effect, as they do on secretion. Previous studies have indicated that store-operated Ca^{2+} entry (SOCaE) is independent of microtubule disassembly (Gregory and Barritt, 1996; Ribeiro et al., 1997). Breakdown of the actin cytoskeleton has been reported to inhibit SOCaE (Holda and Blatter, 1997), whereas other work indicated that the coupling mechanism could withstand actin disassembly (Ribeiro et al., 1997). With the availability of new means to manipulate the actin cytoskeleton, opportunities arose for evaluating the validity of a trafficking model for SOC activation.

We report here that in situ modification of the actin cytoskeleton provides important information on the nature of the coupling between Ca^{2+} stores and PM entry channels. Redistribution of actin into a tight cortical layer subjacent to the PM by induction of actin polymerization or by phosphatase inhibition prevents coupling between ER and PM Ca^{2+} entry channels, while not

*To whom correspondence should be addressed (e-mail: dgill@umaryland.edu).

affecting chemical coupling mediated by $InsP_3$ to release stored Ca^{2+}. Moreover, disassembly of the cortical actin layer so induced permits reestablishment of coupling to activate Ca^{2+} entry. These results indicate that a physical actin barrier, while permitting transmission of the diffusible message mediated by $InsP_3$, prevents a close interaction between ER and the PM that is required to activate Ca^{2+} entry. We suggest that close interactions, while required for SOC activation, do not represent a permanent coupling assembly, but rather a reversible interaction between ER and the PM. We further suggest that the slow activation of Ca^{2+} entry involves a trafficking/translocation event with close parallels to the events mediating secretion, a conclusion compatible with the results of Yao et al. (1999) in this issue of *Cell*.

Results and Discussion

Substantial Breakdown of the Actin Cytoskeleton Does Not Alter Receptor-Mediated Ca^{2+} Store Release or Ca^{2+} Entry Activated by Ca^{2+} Store Depletion

Cytochalasin D (CytD) is a widely utilized membrane-permeant inhibitor of actin polymerization, inducing profound alterations in cellular morphology due to stress fiber disassembly (Cooper, 1987). The effects of CytD-induced actin fiber disassembly on Ca^{2+} signaling in two different cell lines are shown in Figures 1 and 2. The DDT_1MF-2 transformed smooth muscle cell line has been used to study many details of the function and distribution of Ca^{2+} stores and the Ca^{2+} entry activated by store emptying (Ghosh et al., 1989, 1990; Ufret-Vincenty et al., 1995; Gill et al., 1996; Favre et al., 1998). Using fura-2-loaded DDT_1MF-2 cells, emptying of Ca^{2+} stores by the Ca^{2+} pump blocker thapsigargin (TG) was rapid followed by a clear second peak of Ca^{2+} due to SOCaE (Figure 1A). In the absence of extracellular Ca^{2+}, this second peak was absent, the single peak (Figure 1B) reflecting only TG-induced release of Ca^{2+} from stores. Activation of the phospholipase C–coupled bradykinin (BK) receptor gave a faster, $InsP_3$-mediated release of stored Ca^{2+} (Figure 1E). Unlike TG, the receptor-induced response was short-lived, reflecting rapid receptor desensitization and refilling of stores before significant Ca^{2+} entry occurred. The distribution of actin and Ca^{2+}-pumping ER in normal DDT_1MF-2 cells is shown in Figure 1H. Typical prominent actin stress fibers stained with FITC-phalloidin (green) were observed. Immunostaining with SERCA 2b Ca^{2+} pump antibody (red) revealed that Ca^{2+}-pumping ER was widely distributed within the extranuclear cytoplasm.

After 3 hr treatment with 1 μM CytD, cells underwent considerable change. Stress fibers were no longer visible, although small areas of tightly bundled actin remained (Figure 1I). F- and G-actin levels were similar in normal cells (Figure 1H), whereas after CytD treatment G-actin predominated (Figure 1I). Stress fiber disappearance caused substantial change in cell shape; however, SERCA protein remained well distributed. Importantly, neither Ca^{2+} store release nor SOCaE was modified by this extensive cytoskeletal alteration. As shown in Figure 1C, TG-induced Ca^{2+} store release and the ensuing entry of Ca^{2+} were unchanged. Thus, the ER-derived message to activate SOCs as a result of store depletion was functioning normally. Ca^{2+} release activated by BK was also unchanged (Figure 1F). Therefore, the message from the PM mediated by $InsP_3$ to activate ER Ca^{2+} release channels was also operating normally. The cell-permeant sponge toxin latrunculin A (LatA), another powerful blocker of actin polymerization through binding to actin monomers, also induced rapid stress fiber breakdown within DDT_1MF-2 cells (Figure 1J). Again, the toxin-induced disruption had no significant effect on the action of either TG (Figure 1D) or BK (Figure 1G).

Cells vary widely in the amount and distribution of cytoskeleton. DDT_1MF-2 cells exhibit cytoskeletal content and organization typical of fast-growing transformed cells. Whether a more organized cytoskeletal architecture resulted in a distinct relationship between cytoskeletal modification and Ca^{2+} signaling was addressed by comparing a different cell line. Cells of the nontransformed A7r5 smooth muscle line derived from rat embryonic aorta retain much of the morphology and cytoskeletal makeup of primary smooth muscle cells. Phalloidin labeling revealed a dense organized network of actin stress fibers (Figures 2D and 2E) throughout the cytoplasm. Three hours treatment with 1 μM CytD induced almost complete stress fiber disappearance (Figure 2G); the F-actin content of cells appeared to be greatly reduced (Figure 2G) compared to control cells (Figure 2D). Again, CytD caused tightly condensed actin bundles as well as larger areas of condensed actin in some cell extremities (Figure 2G), typically observed in other cells (Cooper, 1987). The binding of CytD to actin filament ends not only stops polymerization but induces dissociation of actin filaments from PM-binding proteins, allowing contraction into tight "foci" (Cooper, 1987). The tight aggregates of actin filaments formed with CytD were resistant to extraction so that few "free" actin filaments remained (Figure 2G). Thus, whereas CytD induced some depolymerization, the predominant effect was to induce filament dissociation from the PM. As with DDT_1MF-2 cells, receptor-activated Ca^{2+} release, in this case, vasopressin (VP), was almost unchanged after CytD treatment; likewise, TG-induced SOCaE was also virtually identical to control cells (Figures 2A and 2B). The lack of effect of CytD on Ca^{2+} entry agrees with the results of Ribeiro et al. (1997), although it was earlier reported that some reduction of Ca^{2+} entry occurred with 20 μM CytD (Holda and Blatter, 1997). In the present study, 1 μM was sufficient to completely disrupt the cytoskeleton and in two cell types induce no alteration of SOCaE up to 10 μM; higher CytD levels can induce actin-independent changes (Matthews et al., 1997). LatA treatment of A7r5 cells resulted in almost identical cytoskeletal changes (Figure 2H), and again there was no change in either release or entry of Ca^{2+} (data not shown). After actin depolymerization with either CytD (Figure 2G) or LatA (Figure 2H), the distribution of ER still appeared widespread.

The results with CytD and LatA are important. Both agents induced complete disassembly of the actin cytoskeleton and substantial alteration in cell morphology, yet Ca^{2+} signal responses were unaltered. If Ca^{2+} entry is mediated by direct coupling, then the coupling must withstand the drastic PM reorganization induced by actin breakdown. The work of Kiselyov et al. (1998) suggests Ca^{2+} entry channel activation can be reconstituted

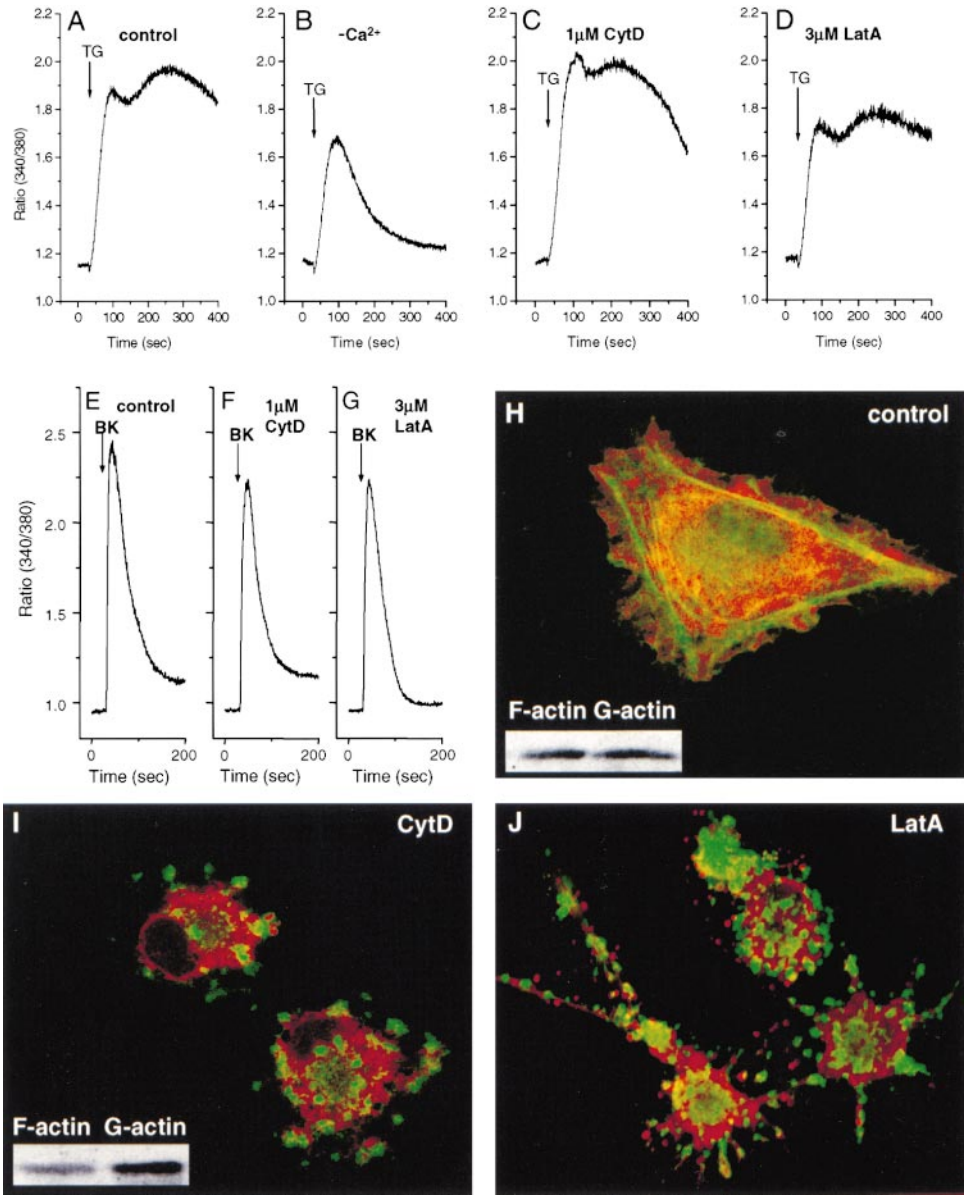

Figure 1. Receptor-Activated Ca^{2+} Store Depletion and Store-Operated Ca^{2+} Entry in DDT_1MF-2 Cells Are Unchanged after Disassembly of the Actin Cytoskeleton

(A–D) Free Ca^{2+} measurements in cells after Ca^{2+} pools were depleted with 1 μM TG (TG; arrow) in normal (1 mM) Ca^{2+} medium (A), in nominally Ca^{2+}-free medium (B), or in normal Ca^{2+} medium after 3 hr treatment of cells with 1 μM cytochalasin (CytD) (C), or in normal Ca^{2+} medium after 1 hr treatment with 3 μM LatA (D).

(E–G) Receptor-induced Ca^{2+} pool release was activated with 10 μM BK (arrow) in the presence of normal 1 mM Ca^{2+} either without pretreatment (E), after treatment with 1 μM CytD for 3 hr (F), or 3 μM LatA for 1 hr (G).

(H–J) Confocal microscopy of DDT_1MF-2 cells stained with FITC-phalloidin (green) and SERCA-2b antibody (red), under the same conditions as for Ca^{2+} measurements: control conditions (H); treatment of cells with 1 μM CytD for 3 hr (I); treatment with 3 μM LatA for 1 hr (J). Insets in (H) and (I) show Western blots of F-actin and G-actin in cells under the same conditions.

by direct addition of ER vesicles to excised PM patches, indicating a direct but *reversible* coupling process. We considered that reversible coupling might fit with a trafficking model involving movement of ER to interact with the PM. It is well established that disassembly of cortical F-actin with CytD *increases* secretion by permitting the approach and docking of secretory vesicles with the PM (Trifaro et al., 1997). Conversely, polymerization and stabilization of cortical actin by introduction of phalloidin into cells prevents the interaction of secretory vesicles with the PM, inhibiting secretion (Muallem et al., 1995). We therefore sought to investigate a secretion-based coupling model for SOC activation by attempting to polymerize cortical actin in situ.

Induction of Actin Polymerization at the Cell Periphery Prevents Ca^{2+} Entry Activated by Ca^{2+} Store Depletion

The cell-permeant cyclic peptide jasplakinolide (JP) isolated from the marine sponge *Jaspis johnstoni* provides

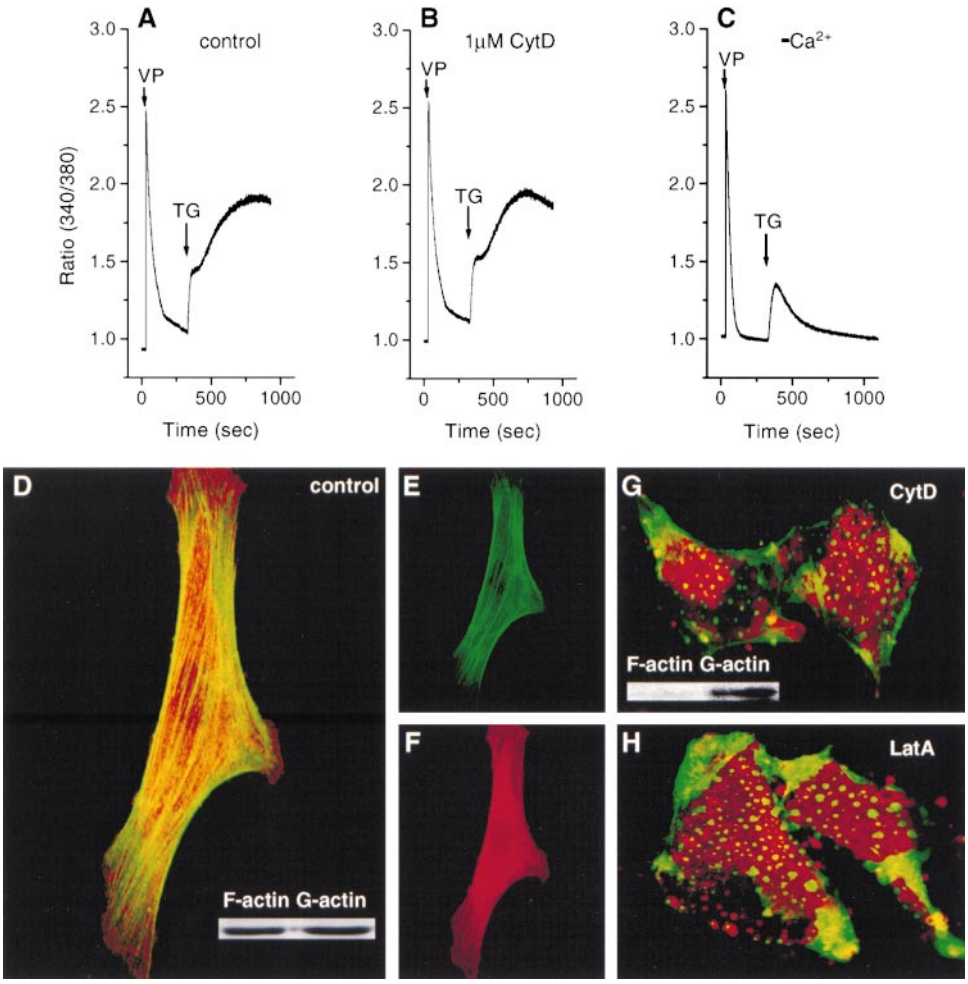

Figure 2. Disassembly of the Actin Cytoskeleton in A7r5 Cells Does Not Alter Receptor-Activated Ca^{2+} Store Depletion or Store-Operated Ca^{2+} Entry

(A–C) Cells were treated with 100 nM VP (first arrow), followed by 1 μM TG (second arrow) in normal 1 mM Ca^{2+} medium (A and B) or nominally Ca^{2+}-free medium (C). Cells were treated for 3 hr with (B) or without (A and C) 1 μM cytochalasin D (CytD).

(D–H) Confocal microscopy of A7r5 cells stained with FITC-phalloidin (green) and SERCA-2b antibody (red) under the same conditions as for Ca^{2+} measurements: control conditions (D–F; green and red channels separated in [E] and [F], respectively, are of the same single cell); treatment of cells with 1 μM CytD for 3 hr (G); treatment with 3 μM LatA for 1 hr (H). Insets in (D) and (G) show Western blots of F-actin and G-actin in cells under the same conditions.

a tool for inducing polymerization and stabilization of actin filaments without microinjection (Bubb et al., 1994). Its actin-binding site and mode of inducing polymerization are highly akin to its membrane-impermeant structural analog, phalloidin (Bubb et al., 1994; Matthews et al., 1997). Significantly, JP prevented Ca^{2+} entry activated by Ca^{2+} store depletion. This effect was observed in both DDT_1MF-2 cells and A7r5 cells (Figure 3). In both cell types, treatment for 60 min with 3 μM JP was sufficient to prevent SOCaE. After JP treatment of DDT_1MF-2 cells, the cytosolic Ca^{2+} response to TG was only release of Ca^{2+} (Figures 3A and 3C), a response little different to that observed with control cells in the absence of external Ca^{2+} (Figure 3B). JP had no significant effect on resting cytosolic Ca^{2+} levels, nor any effect on the size of the Ca^{2+} store released with TG. Although Ca^{2+} entry was more sustained in A7r5 cells, treatment for 60 min with 3 μM JP again almost eliminated entry (Figure 3G) but had no effect on VP-activated Ca^{2+} release (Figures 3F and 3G). As with BK on DDT_1MF-2 cells, the VP receptor undergoes fast desensitization, resulting in rapid turn off of $InsP_3$ production, refilling of stores, and hence little Ca^{2+} entry. The results show that the chemical coupling between receptor and Ca^{2+} stores mediated by $InsP_3$ is not changed by JP, whereas the coupling from stores back to the PM to activate Ca^{2+} entry is blocked.

The structural changes induced in cells by JP were quite distinct from those induced by CytD or LatA. Morphologically, cells took on a more rounded appearance but remained attached. After 60 min with 3 μM JP, F-actin underwent a clear change in distribution in DDT_1MF-2 cells (Figure 3E). Stress fibers (Figure 3D) were no longer apparent, and F-actin became organized almost exclusively at the cell periphery. SERCA pump remained well distributed after JP treatment; however, there was little overlap (yellow) of actin-rich areas and areas containing SERCA pump in the JP-treated cell

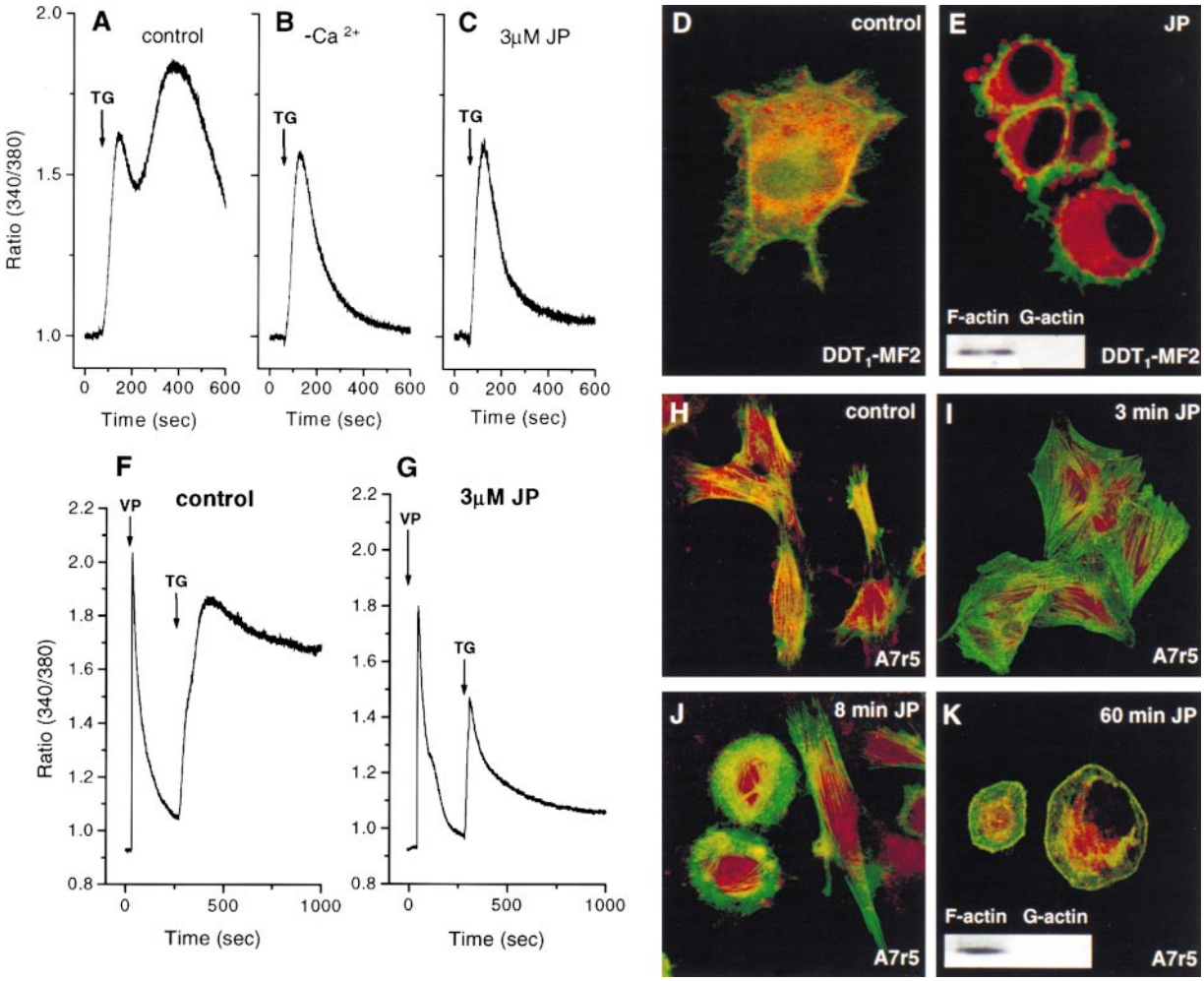

Figure 3. Polymerization and Reorganization of F-Actin Induced by the Cell-Permeant Phalloidin Analog, Jasplakinolide, Prevents Store-Operated Ca^{2+} Entry but Does Not Affect Receptor-Activated Ca^{2+} Pool Depletion

(A–C) Ca^{2+} pools were depleted in DDT_1MF-2 cells with 1 μM TG (arrow), in normal (1 mM) Ca^{2+} medium (A), in nominally Ca^{2+}-free medium (B), or in normal Ca^{2+} medium after treatment of cells with 3 μM JP for 1 hr (C).

(D and E) Confocal microscopy of DDT_1MF-2 cells stained with FITC-phalloidin (green) and SERCA-2b antibody (red) under the same conditions as for Ca^{2+} measurements: control conditions (D); cells treated with 3 μM JP for 1 hr (E).

(F and G) A7r5 cells were treated with 100 nM VP (first arrow), followed by 1 μM TG (second arrow) in normal 1 mM Ca^{2+} medium after treatment either without (F) or with 3 μM JP for 1 hr (G).

(H–K) Confocal microscopy of A7r5 cells stained as above under the same conditions as for Ca^{2+} measurements: control conditions (H), cells treated with 3 μM JP for 3 min (I), cells treated with 3 μM JP for 8 min (J), or cells treated with 3 μM JP for 1 hr (K).

(E and K, insets) Western blots of F-actin and G-actin in respective cells.

images (Figure 3E). JP-induced promotion of actin polymerization was clear from analysis of the relative abundance of F- and G-actin; virtually no G-actin was detectable (Figure 3E). Although phalloidin does not enter cells, microinjection or addition to permeabilized cells causes elongation of existing actin filaments and induction of new filaments, predominantly near the PM (Cooper, 1987). Such effects are consistent with enhanced formation of peripheral F-actin by JP seen in DDT_1MF-2 cells (Figure 3E). JP induced similar F-actin changes in A7r5 cells (Figures 3H–3K). Normal cells exhibited widely distributed ER with much overlapping staining of actin filaments (yellow predominated in Figures 2D and 3H). By 3 min with JP, there was increased labeling intensity of stress fibers (Figure 3I) consistent with JP-induced elongation of F-actin seen in other cells (Shurety et al., 1998). After 8 min, some cells had continued to develop F-actin toward the periphery and had rounded, whereas others still retained stress fibers (Figure 3J). Between 30 and 60 min of treatment, all G-actin had been converted to F-actin and cells had developed a ring of actin close to the PM (Figure 3K). In JP-treated A7r5 cells, SERCA-labeled ER appeared more centrally located, perhaps due to thinning of cells toward the periphery (Figures 3I–3K). Following JP treatment of DDT_1MF-2 cells (Figure 3E), ER was evenly distributed throughout the cytoplasm, with the exception of the peripheral actin layer. Thus, the single morphological criterion that was consistent in the two cell types was the JP-induced development of a dense ring of actin filaments close to

the PM, which appeared to exclude ER from the PM vicinity.

From these results there is a clear divergence in the action of JP on receptor-induced Ca^{2+} release as opposed to Ca^{2+} entry activated by store depletion. Thus, the well-defined PM-originating chemical message, $InsP_3$, was able to function normally to stimulate Ca^{2+} release channels in the ER. Yet the message originating from the ER to activate PM Ca^{2+} entry channels was interrupted. If the peripheral dense ring of actin induced by JP was the correlative factor, we reasoned that this may be preventing a close interaction between ER and PM necessary for SOC activation. Injected into cells, phalloidin stabilizes cortical actin and prevents the interaction of secretory vesicles with the PM (Muallem et al., 1995; Becker and Hart, 1999). In contrast, CytD enhances secretion by disassembling cortical actin, allowing secretory vesicles access to the PM (Muallem et al., 1995; Becker and Hart, 1999). JP, like phalloidin, has been observed to prevent secretion, and this effect has been ascribed to cortical actin barrier formation at the PM (Carbajal and Vitale, 1997; Matthews et al., 1997). In ultrastructural studies, JP-induced actin polymerization causes bunching of actin close to the PM and can exclude cytoplasmic organelles from this region (Shurety et al., 1998). Therefore, there is clearly precedent for the action of actin polymerization in preventing close association between the PM and internal organelles.

F-Actin Association with the Plasma Membrane Induced by Phosphatase Inhibition Prevents Store-Operated Ca^{2+} Entry

By analogy with secretion, a model began to emerge whereby actin filaments might prevent the interaction between ER and the PM necessary for activation of Ca^{2+} entry. Important to determine was an independent means of assessing whether actin could interfere with the coupling process. Much new information has emerged on the structure, function, and regulation of actin-binding proteins involved in cross-linking actin filaments with the PM. Prominent among these are the ezrin, radixin, and moesin (ERM) family of proteins, which are powerful mediators of actin cross-linking to the PM (Tsukita et al., 1997). The C-terminal portion of ERM proteins interacts with actin, while conserved sequences in the N-terminal domain interact with integral PM proteins (Amieva et al., 1999). Phosphorylation of specific threonine residues conserved in the C-terminal region activates the interaction of ERM proteins with the PM (Matsui et al., 1998; Pietromonico et al., 1998), and this can be mediated by Rho kinase (Mackay et al., 1997; Matsui et al., 1998) or protein kinase Cθ (Pietromonico et al., 1998). A highly effective means of inducing phosphorylation-dependent association of the actin-binding ERM proteins with the PM is through use of the serine/threonine phosphatase inhibitors, okadaic acid (OA) and calyculin A (calyA). CalyA specifically blocks PP1 and PP2A phosphatases in intact cells with a potency 10- to 100-fold greater than OA due to its higher PM permeation (Favre et al., 1997). Both phosphatase inhibitors induce major cytoskeletal reorganization; normal stress fibers disappear rapidly and actin filaments become redistributed. In many cells, actin becomes tightly condensed at the PM (Kreienbuhl et al., 1992; Downey et al., 1993; Hosoya et al., 1993; Shinoki et al., 1995). In addition, condensed actin bundles can be seen inside cells (Shinoki et al., 1995; Toivola et al., 1997), which may reflect condensation of actin filaments with intermediate filaments (Toivola et al., 1997). Phosphatase inhibition clearly enhances association of ERM proteins with the PM (Chen and Mandel, 1997; Tsukita et al., 1997; Simons et al., 1998) and likely accounts for the observed enhancement of actin binding to the PM.

Importantly, calyA was observed to specifically block SOCaE and to induce cytoskeletal redistribution corresponding closely to that induced by JP. As shown in Figures 4 and 5, calyA induced an almost complete blockade of Ca^{2+} entry activated by store emptying, in agreement with earlier observations of Sakai and Ambudkar (1996). In DDT_1MF-2 cells, the action of calyA was rapid; after treatment with 100 nM calyA for just 10 min, TG-induced SOCaE was almost eliminated (Figures 4A–4C), while the size of the intracellular Ca^{2+} stores was unchanged. CalyA elicited no alteration in resting Ca^{2+} levels (Figure 4C). Analysis of distribution of actin and SERCA-pumping ER (Figures 4D and 4E) revealed a correspondingly rapid redistribution of actin filaments to the cell periphery. By 10 min, stress fibers were no longer observable, but F-actin had condensed into a clearly discernible dense ring close to the PM. The picture was highly reminiscent of the action of JP seen in Figure 3, and again little overlap of ER and actin was observed. As with JP, the distribution of ER within the extranuclear cytoplasm appeared uniform with the exception of its exclusion from the cell periphery where dense F-actin was present (Figure 4E). One clear difference from the action of JP was that calyA did not alter relative amounts of F- and G-actin (Figure 4E). Thus, calyA appeared to activate a translocation of existing F-actin to the cell periphery, independent of polymerization and consistent with the phosphorylation events described above. In contrast, JP increased peripheral actin through induction of polymerization of new (and/or elongation of existing) fibers; thus, inhibition of SOCaE observed with JP was not related to the elimination of G actin. As with both JP and CytD, calyA induced significant morphological changes; cells became more rounded and some PM surface blebs were apparent, likely reflecting stress fiber disappearance. Interestingly, even the surface blebs contained F-actin uniformly associated with the membrane surface (Figure 4E). In other experiments (data not shown) addition of calyA to cells after TG-activated pool emptying resulted in similar cytoskeletal change. Moreover, when added at the time of maximal Ca^{2+} entry following TG (300 s), Ca^{2+} entry was deactivated with a time dependence corresponding to cytoskeletal redistribution. This is significant, indicating that the coupling process for Ca^{2+} entry is not only prevented from being activated but can be *reversed* after activation as a result of redistribution of actin. The calyA sensitivity of both Ca^{2+} entry blockade and reorganization of actin corresponded closely with the calyA sensitivity of phosphatase inhibition (Favre et al., 1997); at 100 nM, the action of calyA was maximal, whereas at 10 nM its effects on Ca^{2+} entry and actin distribution took several hours to develop. OA at 100 nM required overnight incubation but induced the same results; a

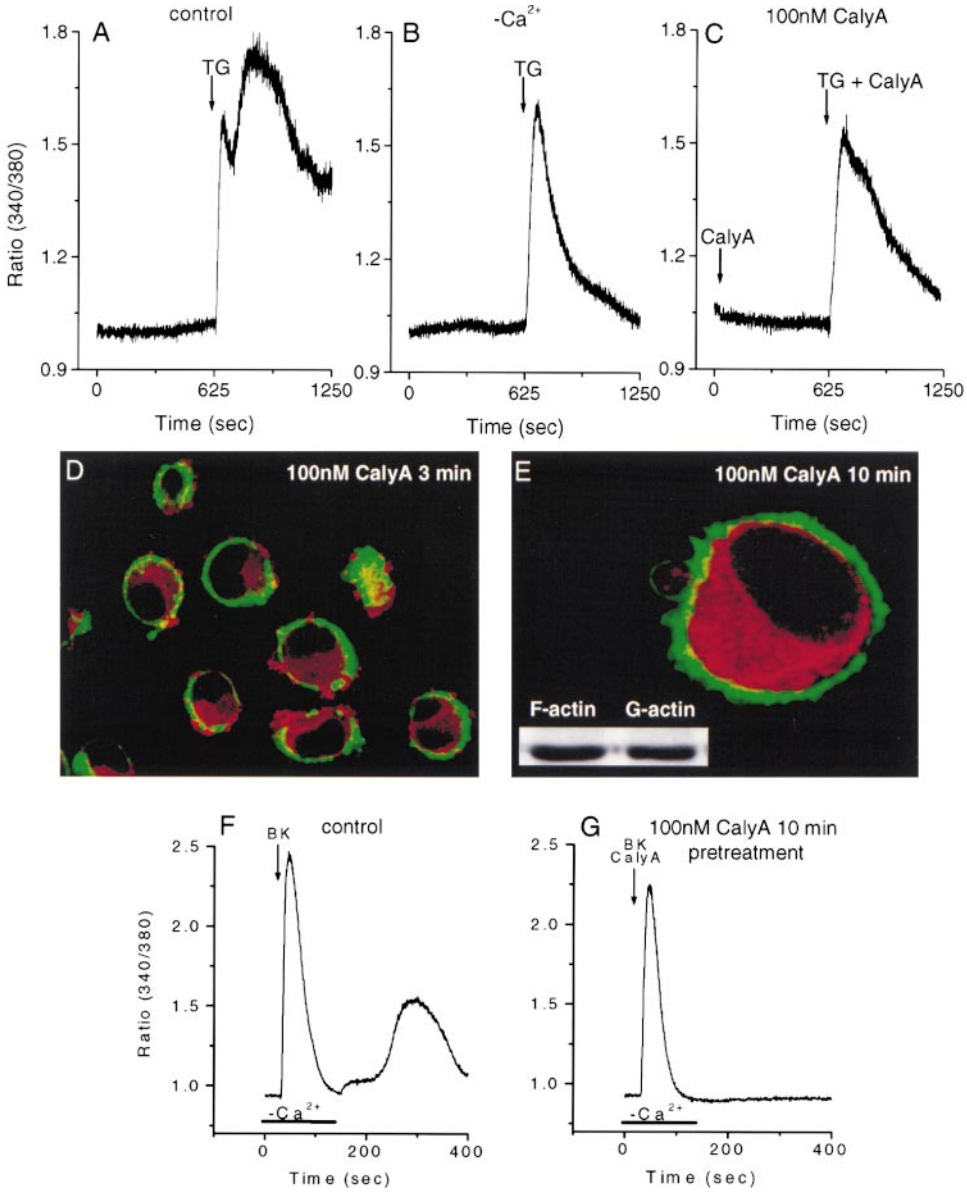

Figure 4. The Phosphatase Inhibitor Calyculin A Promotes F-Actin Redistribution into a Tight Cortical Layer and Prevents Store-Operated Ca^{2+} Entry Activated by Either SERCA Pump Inhibition or Receptor-Activated $InsP_3$ Production in DDT_1MF-2 Cells

(A–C) Ca^{2+} pools were depleted in cells with 1 μM TG (arrow), in normal (1 mM) Ca^{2+} medium (A), or in nominally Ca^{2+}-free medium (B). In (C), 100 nM calyA was added (first arrow), followed 10 min later by addition of 1 μM TG with calyA (second arrow).

(D and E) Confocal microscopy of DDT_1MF-2 cells (stained for F-actin and SERCA pump as in Figure 1) after treatment with 100 nM calyA for either 3 min (D) or 10 min (E). Inset of (E), Western blot of F-actin and G-actin in cells treated with calyA for 10 min.

(F) 10 μM BK (first arrow) was added in nominally free Ca^{2+} medium (bar), followed by replacement with normal (1 mM) Ca^{2+} medium.

(G) As in (F) except 100 nM calyA was added 10 min prior to BK addition. (CalyA was also added with BK as shown.)

third PP1/PP2A phosphatase inhibitor, tautomycin, also induced the same effects but was required at 1 μM for 3 hr. These effects correspond well with the specificity and sensitivity of the agents on phosphatase inhibition (Favre et al., 1997) and suggest that the effects on both Ca^{2+} entry and actin redistribution are a consequence of phosphatase inhibition.

It was also important to assess whether calyA treatment induced any alteration of the chemical message mediated by $InsP_3$ to empty stores. Clearly, BK-induced emptying of stores (measured without external Ca^{2+} to prevent Ca^{2+} entry) remained unchanged after calyA treatment (Figures 4F and 4G). A further question was whether Ca^{2+} entry activated by $InsP_3$-mediated Ca^{2+} release (as opposed to TG) was sensitive to calyA. As shown in Figure 4F, when Ca^{2+} was added back after BK-induced store emptying, a Ca^{2+} entry component was clearly discernible (c.f. in Figure 1, with external Ca^{2+} present, receptor desensitization resulted in store refilling and little Ca^{2+} entry). Without extracellular Ca^{2+},

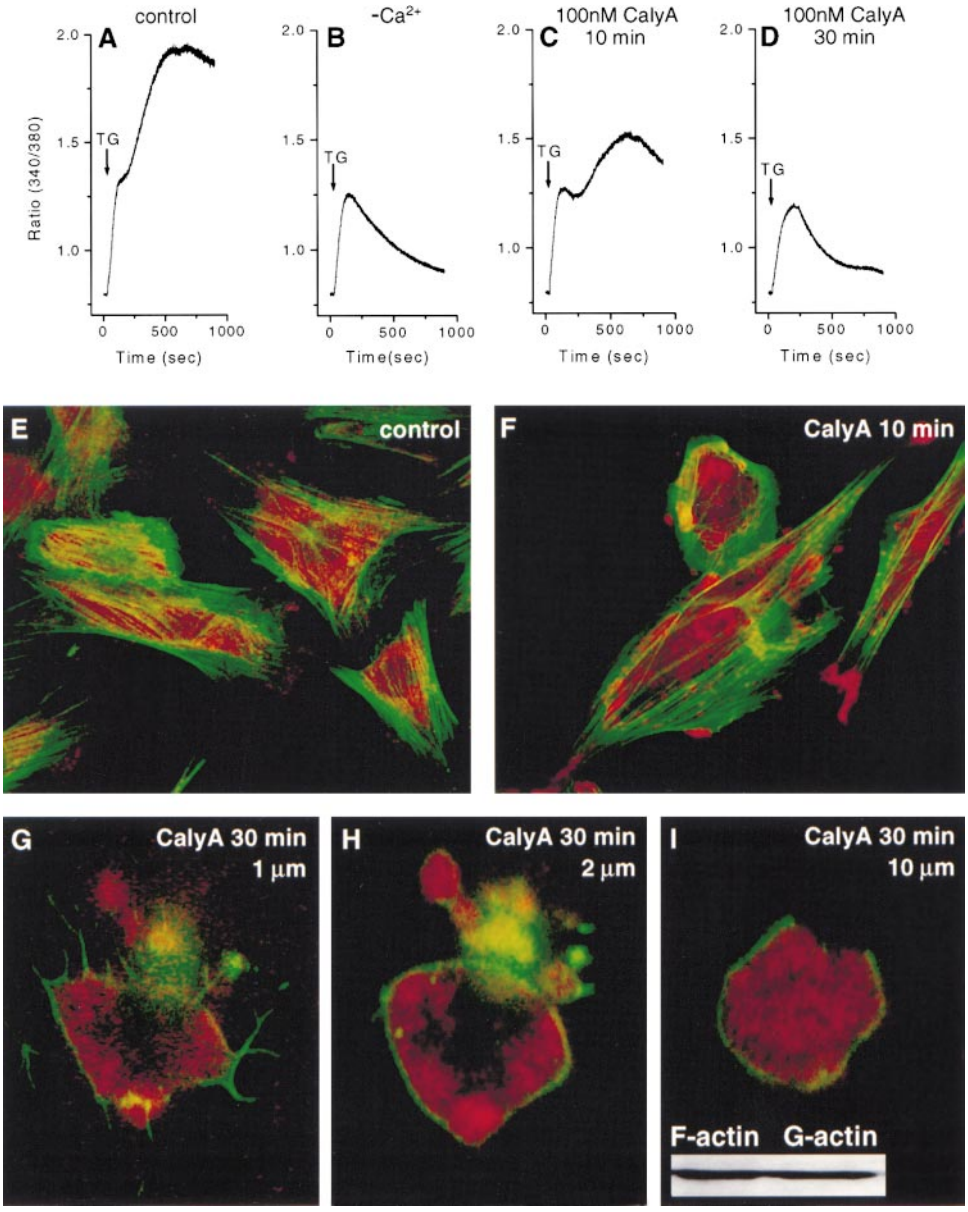

Figure 5. Time Course of Cortical F-Actin Formation in A7r5 Cells Induced by Calyculin A Correlates with Blockade of Store-Operated Ca^{2+} Entry

(A–D) Ca^{2+} pools were depleted in A7r5 cells with 1 μM TG (arrow), in normal (1 mM) Ca^{2+} medium (A), in nominally Ca^{2+}-free medium (B), or in normal Ca^{2+} medium after prior treatment of cells with 100 nM calyA for either 10 min (C) or 30 min (D). When present, 100 nM calyA was maintained after TG addition.

(E–I) Confocal microscopy of normal A7r5 cells (stained for F-actin and SERCA pump as in Figure 2) (E) or cells after treatment with 100 nM calyA for either 10 min (F) or for 30 min (G–I). Images shown in (G)–(I) are serial z-section images of a single cell taken at 1, 2, and 10 μm (as shown) above the plane of attachment. Inset of (I), Western blot of F-actin and G-actin in cells treated with calyA for 30 min.

released Ca^{2+} was pumped out of the cell and stores remained emptied for longer. Thus, in Figure 4F, readdition of Ca^{2+} reflected entry as a result of $InsP_3$-mediated store release (Figure 4F). The slow kinetics of activation of Ca^{2+} entry were similar to those for TG-induced entry, peaking at approximately 300 s. Clearly, 10 min treatment with 100 nM calyA completely blocked Ca^{2+} entry induced by $InsP_3$-mediated store emptying, while not altering the release process (Figure 4G). This provided good evidence for the selectivity of action of calyA to inhibit the ER-derived signal to activate SOCs, while not altering the PM-derived release signal ($InsP_3$) or the size of the stores themselves.

Analysis of the action of calyA on A7r5 cells confirmed its effect on preventing the ER-derived signal for Ca^{2+} entry and provided further evidence that this action resulted from rearrangement of actin. The entry of Ca^{2+} in response to TG-induced Ca^{2+} store release was eliminated in A7r5 cells by 100 nM calyA (Figures 5A, 5B, and 5D). Again, the size and releasability of Ca^{2+} stores

were unaffected by calyA. However, the time course of action of the phosphatase inhibitor on preventing SOCaE in A7r5 cells was different from DDT_1MF-2 cells. Whereas blockade was complete following 30 min exposure to calyA (Figure 5D), the effect was only partial after 10 min exposure (Figure 5C). The time course for inhibition corresponded well with alteration in the redistribution of F-actin in A7r5 cells (Figures 5E–5I). After 10 min, incomplete change in F-actin distribution and cell morphology was observed in some cells (Figure 5F). By 30 min, most cells no longer contained stress fibers, and confocal sectioning revealed a clearly discernible layer of F-actin closely associated with the PM throughout the cell (Figures 5G–5I). CalyA-treated A7r5 cells became more rounded with increased cell height but remained surface attached. Occasional surface blebs were observed and some cells contained discrete areas of condensed F-actin, as described for other cells (Toivola et al., 1997). The longer time for the rearrangement of actin in A7r5 cells likely reflected the much greater content and degree of organization of actin filaments as compared to DDT_1MF-2 cells. Certainly, the time for appearance of this altered F-actin distribution correlated well with disappearance of SOCaE.

Disassembly of Membrane-Associated F-Actin by Cytochalasin D Restores Store-Operated Ca^{2+} Entry

The studies above suggest that formation of a PM-associated layer of F-actin may uncouple store emptying from activation of Ca^{2+} entry by presenting a barrier restricting interaction between ER and the PM. Strength for this conclusion is derived from the observations that two distinct biochemical modifications in two morphologically distinct cell types induced similar cytoskeletal rearrangement, ER displacement, and blockade of Ca^{2+} entry. As described above, the corresponding effects of JP and calyA on actin redistribution and blockade of secretory vesicle interaction with the PM provided some precedent for this model. Whereas the effect of JP likely reflected a selective cytoskeletal action, it would have been naive to consider that the action of phosphatase inhibitors was limited to cytoskeletal modification. Therefore, we sought to provide a more *direct* means to verify the connection between actin reorganization and Ca^{2+} entry. We reasoned that if calyA-induced formation of cortical F-actin caused uncoupling between Ca^{2+} stores and the PM, then prior treatment with CytD, which would cap barbed F-actin ends and prevent their PM attachment (Cooper, 1987), might prevent this uncoupling. As shown in Figures 6A–6C, treatment with CytD indeed prevented the inhibitory action of calyA. Thus, if DDT_1MF-2 cells were treated for 3 hr with 1 μM CytD to completely dissociate the cytoskeleton, the addition of 100 nM calyA for 10 min no longer inhibited Ca^{2+} entry (Figure 6C). Cells preincubated for the same 3 hr period without CytD retained full sensitivity to calyA (Figure 6B). The result has added significance, since CytD per se does not alter any measurable aspect of Ca^{2+} signaling (see Figures 1 and 2). Nor would it be expected that CytD would prevent a phosphorylation event that might have blocked SOCaE independent of cytoskeletal change. Therefore, we suggest that the action of calyA on Ca^{2+} entry is mediated by cytoskeletal modification.

Nevertheless, we considered a yet more direct approach to this question. If calyA-induced blockade of Ca^{2+} entry activation truly resulted from the presence of reorganized cortical actin, then if CytD could dissociate the relocated actin we expected to see reappearance of Ca^{2+} entry. The distribution of cytoskeleton and ER under such conditions was carefully examined (Figures 6D–6F). Initially we examined whether the effect of calyA on cytoskeletal reorganization was spontaneously reversible. As shown in Figure 6D, treatment of cells for 10 min with 100 nM calyA followed by removal of calyA for 30 min did not result in loss of the tight peripheral ring of actin, nor any obvious change in the dispersal of SERCA-labeled ER or its penetration within the excluded actin-containing area. Indeed, continued incubation for up to 3 hr following removal of calyA did not significantly reverse actin distribution. However, if calyA-treated cells were exposed to 5 μM CytD, redistribution of actin was observed within 30 min (Figures 6E and 6F). CytD induced a similar actin distribution to that observed in Figure 1 for normal cells. The continuous peripheral cortical actin layer was no longer visible, and dense centralized actin bodies, typical of the action of CytD appeared within cells predominantly in the lower plane of cells (Figure 6E). SERCA-labeled ER remained well distributed. Indeed, at higher elevations within the cells, ER clearly extended throughout the cytoplasmic space and was not excluded from the areas subjacent to the membrane (Figure 6F). The clearly defined peripheral ring of actin consistently observed with calyA was absent. CalyA followed by prolonged (3 hr) CytD treatment posed a harsher condition (manifested as cell detachment from coverslips) compared to the reversed order of addition, hence the use of higher CytD (5 μM) for a shorter time period (25 min).

Importantly, recovery of SOCaE was observed following CytD treatment of the calyA-treated cells. Reappearance of SOCaE occurred only in calyA-treated cells following exposure to CytD (Figure 6I) and not in cells treated identically but not exposed to CytD (Figure 6H). Although Ca^{2+} entry was not restored to 100% of entry seen with cells exposed to neither modifier (Figure 6G), a substantial increase in Ca^{2+} entry was observed in 5 out of 5 independent experiments, with no significant change in resting Ca^{2+} levels or size of releasable stores (Figure 6I). CytD-induced restoration of the coupling mechanism activating Ca^{2+} entry, and its correlation with an observed cytoskeletal rearrangement corresponding to the established actin-modifying action of CytD, provides an independent verification of the hypothesis that coupling between stores and the PM is mediated by a close physical interaction. Moreover, it indicates that the process of preventing coupling as a result of actin reorganization is a reversible phenomenon and that the machinery for coupling can be disassembled and reassembled.

Lastly, experiments were also conducted to test any modification or reversal of the action of JP by CytD (data not shown). Following CytD treatment, addition of JP caused some reorganization of actin, and its reduction of Ca^{2+} entry was diminished but not prevented. The

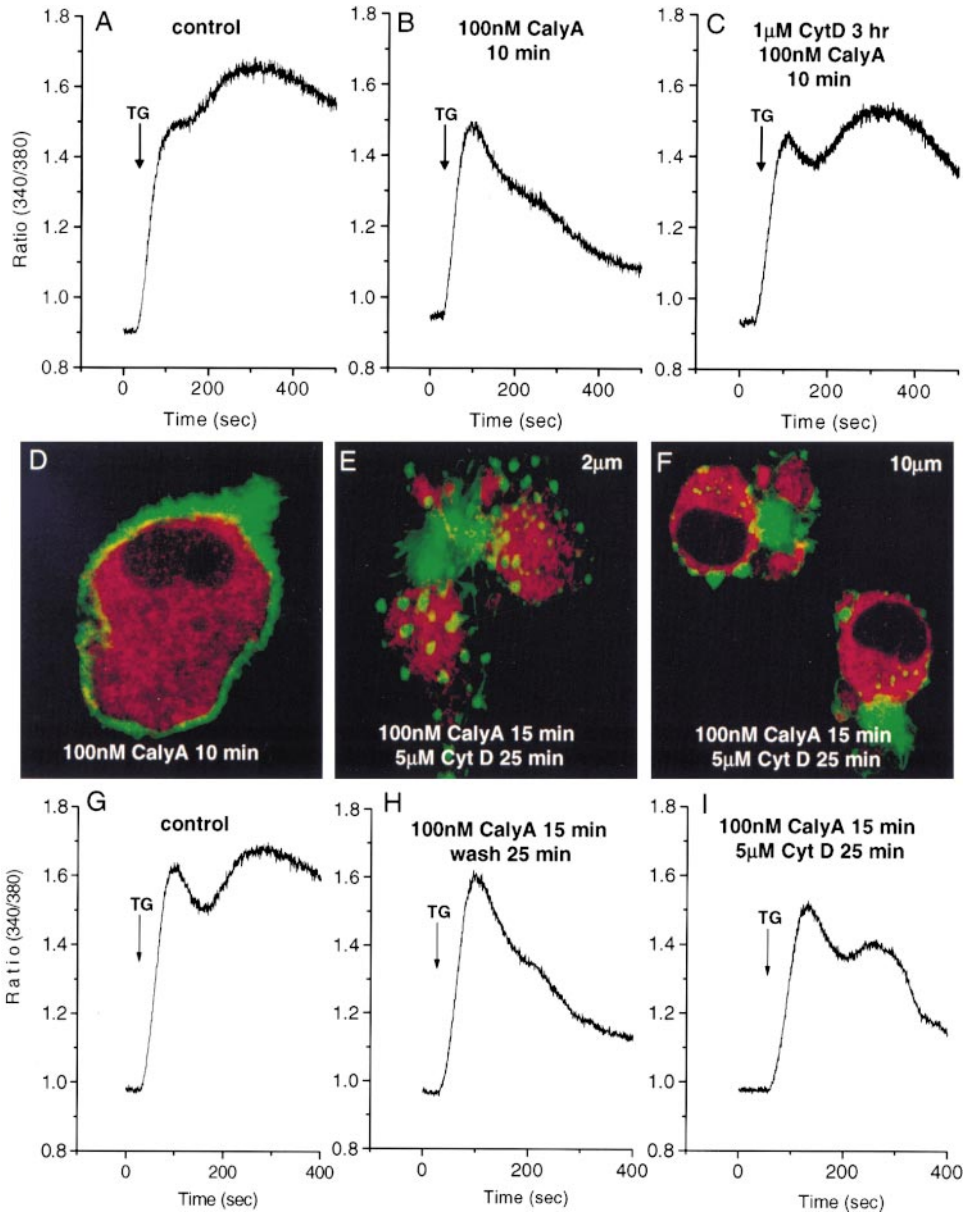

Figure 6. Disassembly of the Calyculin A–Induced Dense Cortical Actin Layer Permits Return of ER Access to the Plasma Membrane and Reverses the Blockade of Store-Operated Ca^{2+} Entry

(A–C) Ca^{2+} pools were depleted in DDT_1MF-2 cells with 1 μM TG (arrow), in normal (1 mM) Ca^{2+} medium (A), or in normal Ca^{2+} medium after prior treatment of cells with 100 nM calyA for 10 min (B). In (C), cells were treated for 3 hr with 1 μM CytD, then treated for 10 min with calyA, exactly as in (B).

(D–F) Confocal microscopy of DDT_1MF-2 cells (stained for F-actin and SERCA pump as in Figure 1) after treatment with 100 nM calyA for 10 min (D) or after treatment with 100 nM calyA for 15 min followed by 5 μM CytD for 25 min (E and F). (E) and (F) are confocal images of different cells taken at either 2 μm or 10 μm (as shown) above the plane of cell attachment.

(G–I) Ca^{2+} pools were depleted in normal DDT_1MF-2 cells with 1 μM TG (arrow), in normal (1 mM) Ca^{2+} medium (G), or in normal Ca^{2+} medium after prior treatment of cells with 100 nM calyA for 15 min followed by either wash with normal Ca^{2+} medium for 25 min (H) or addition of 5 mM CytD in normal Ca^{2+} medium for 25 min (I).

potent polymerizing action of JP may partially overcome the effect of CytD. In the converse experiment, the action of JP to assemble cortical actin and block store-operated Ca^{2+} release in neither case could be reversed by even prolonged CytD treatment, a result consistent with the high binding affinity of JP for F-actin (K_D = 15 nM), reportedly even greater than that of phalloidin (Bubb et al., 1994). Indeed, this provides evidence that the action of CytD to induce recoupling of store-operated entry after calyA is specifically due to actin disassembly and is not observed when blockade of coupling is mediated by an essentially irreversible actin-polymerizing agent.

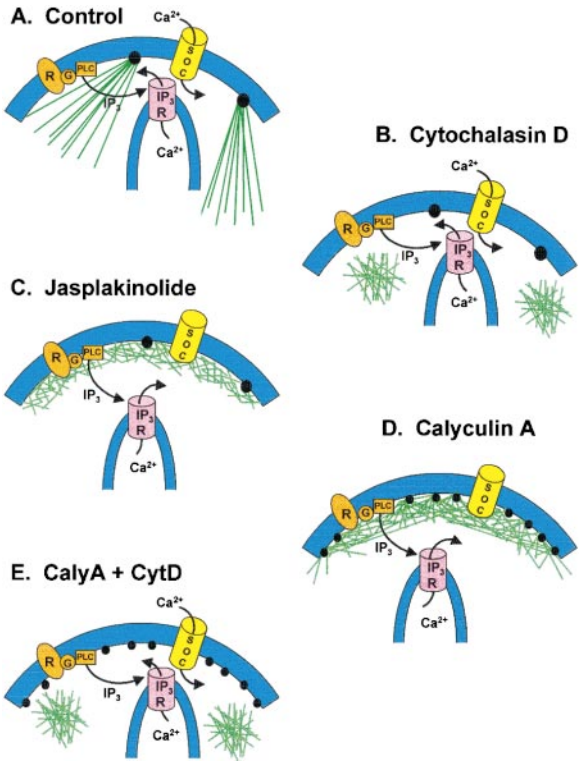

Figure 7. Model for Cytoskeletal Restructuring and Effects on Ca^{2+} Signal Generation

(A) Ca^{2+} signaling in normal cells: coupling occurs independently of F-actin fibers shown emanating from PM attachment sites.

(B) CytD-induced reorganization of PM actin into dense foci does not modify $InsP_3$-induced Ca^{2+} release or SOCaE.

(C) Actin polymerization by JP induces a tight cortical actin band, displacing cortical ER and blocking SOCaE; $InsP_3$-mediated Ca^{2+} release is unaffected.

(D) CalyA relocates F-actin to the PM (likely by activation of PM-attached actin-linking proteins), with effects similar to JP.

(E) CytD disassembles tight cortical actin assembled by calyA, reestablishing ER–PM coupling and SOC activation.

Concluding Discussion

The activation of Ca^{2+} entry channels following Ca^{2+} store release is a signaling mechanism of great significance, yet the mechanism by which such channels become activated has remained a mystery. Predominant theories centered on either a diffusible messenger released from ER or a direct coupling mechanism involving physical connections between ER and PM. Through application of novel means to restructure the cytoskeleton, our results provide some important perspectives on the nature of the coupling process. Figure 7 provides a summary of the cytoskeletal modifications and their effects on Ca^{2+} signal generation. The results derive particular significance from comparing the effects of cytoskeletal changes on both of the two phases of the Ca^{2+} signaling response: the Ca^{2+} release signal from PM to ER, and the Ca^{2+} entry signal from ER back to the PM.

None of the modifications to cytoskeletal structure or distribution altered the $InsP_3$-mediated signaling step. Neither elimination of actin filaments from the vicinity of the PM with CytD nor the formation of dense actin filament networks subjacent to the PM induced by JP or calyA altered the Ca^{2+} release signal. This indicates that the chemically mediated message is neither dependent on nor hindered by actin filaments. Moreover, considering the evidence that actin reorganization displaces ER from the vicinity of the PM, the chemical release message appears independent of the distance between the two membranes. These results contrast distinctly from the actions of cytoskeletal reorganization on coupling between the ER and the PM to activate Ca^{2+} entry. In this case, formation of a physically discernible F-actin barrier blocks coupling, and removal of the barrier allows reestablishment of coupling. Based on the comparable effects of cytoskeletal rearrangement on secretory vesicle interaction with the PM (Trifaro et al., 1997), a "secretion-like" coupling model for SOC activation is invoked. Since removal of actin with CytD neither promotes nor inhibits coupling, the model does not include a role of actin filaments in driving or stabilizing the coupling process.

In contrast with earlier models for SOC activation, we conclude that coupling is mediated by neither a diffusible chemical mediator nor a permanently assembled junctional unit. Instead, we propose a slowly activating trafficking event akin to the early events in secretion, but culminating in a close interaction or docking process, not necessarily membrane fusion. Such a model is most compatible with the recent work of Yao et al. (1999), suggesting SOC activation in *Xenopus* oocytes is mediated by trafficking. In this work, physically induced separation of the PM from internal stores (akin to the effects of cortical actin described here) prevented activation. Ca^{2+} entry activation was suppressed by Rho A GTPase, perhaps reflecting Rho kinase–induced reorganization of actin. Also, blockade of Ca^{2+} entry with dominant-negative mutants of SNAP-25 implicated a role of the exocytotic docking machinery in SOC activation.

Clearly, the well-documented slow activation of Ca^{2+} entry following store release is consistent with a trafficking model (Hoth and Penner, 1993; Zweifach and Lewis, 1993; Parekh and Penner, 1997; Kerschbaum and Cahalan, 1999). Independent support for the model is provided from the evidence that GTPγS blocks SOC activation (Bird and Putney, 1993; Fasolato et al., 1993; Somasundaram et al., 1995; Fernando et al., 1997; Parekh and Penner, 1997), an effect overcome by addition of GTP (Bird and Putney, 1993; Fasolato et al., 1993; Parekh and Penner, 1997). This strongly implicates a GTP-binding protein–mediated event dependent on GTP hydrolysis and likely involving membrane trafficking. Once SOC coupling has been activated, GTPγS appears no longer to block (Bird and Putney, 1993; Fasolato et al., 1993; Parekh and Penner, 1997), signifying a relatively long-lasting coupling interaction. Although the fusion inhibitor primaquine was reported to block Ca^{2+} entry (Somasundaram et al., 1995), this effect was later reported to be unrelated to membrane fusion (Gregory and Barritt, 1996). Our results on reversal and reestablishment of the coupling process by actin reorganization, together with the recent reconstitution evidence from Kiselyov et al. (1998), support the view that fusion is not necessary. Based on these facts, it is important to recall that in permeabilized cells, ER membranes containing functional $InsP_3$ receptors undergo a membrane-coupling process activated by GTP, blocked by GTPγS, and

dependent on GTP hydrolysis (Gill et al., 1993, 1996; Rys-Sikora et al., 1994; Rys-Sikora and Gill, 1998). Although the target membrane was never identified as PM, the coupling was characterized as a relatively long-lasting G protein–mediated docking process permitting Ca^{2+} transport, which, once activated, was not reversed with GTPγS (Ghosh et al., 1989; Gill et al., 1993). However, the GTP-dependent docking and communication could be fully reversed by fatty acyl CoA derivatives, providing strong evidence that membrane fusion had not occurred and was not necessary for the process (Rys-Sikora et al., 1994; Rys-Sikora and Gill, 1998). Indeed, even secretory vesicles need not necessarily fuse in order to permit release (Neher, 1993), and switching of secretion to the "kiss and run" mode of operation appears dependent on local Ca^{2+} levels (Alés et al., 1999). We hypothesize that the parallel between secretory events and the SOC activation may be even stronger than the evidence thus far presented.

Experimental Procedures

Antibodies and Reagents

Anti SERCA-2b monoclonal antibody, MA3-910, was from Affinity Bioreagents Inc. Slo-Fade, FITC-phalloidin, fura-2 AM, and Alexa 546 goat anti-mouse antibody were from Molecular Probes. JP and LatA were generous gifts from Dr. Phillip Crews (University of California, Santa Cruz). TG was from LC Services; CytD and calyA were from Calbiochem; molecular weight standards and enhanced chemiluminescence reagents were from DuPont; orthovandadate, β-glycerophosphate, phenlyalanine, aprotinin, leupeptin, bicinchoninic acid, Triton X-100, polyclonal actin antibody (A-2066), goat serum, phenlymethylsulfonyl fluoride (PMSF), saponin, BK, paraformaldehyde, VP, and dithiothreitol were from Sigma.

Cells and Intracellular Calcium Measurements

Culture and cytosolic Ca^{2+} measurements for DDT_1MF-2 and A7r5 cells were as previously described (Ufret-Vincenty et al., 1995; Favre et al., 1998). Resting Ca^{2+} levels in both cell lines were approximately 60–100 nM. Measurements shown are representative of at least three and in most cases a larger number of independent experiments. Treatment with cytoskeletal modifiers was undertaken for times specified at 20°C.

Immunohistochemistry

DDT_1MF-2 and A7r5 cells grown on coverslips for 1 day were fixed with 3% paraformaldehyde in 2× PBS for 30 min and washed three times in 2× PBS for 15 min. Coverslips were quenched in 50 mM NH_4Cl for 15 min and washed three times in 2× PBS for 15 min. Cells were permeabilized in saponin solution (2× PBS, 1% bovine serum albumin, 1% goat serum, and 0.075% w/v saponin) for 1 hr. Coverslips were washed three times in 2× PBS for 15 min and subsequently inverted on 250 μl of antibody/phalloidin solution (SERCA 2b antibody 1:500 with FITC-phalloidin 1:50 in saponin solution) in a wet chamber overnight at 4°C. Since JP binds to the same site as phalloidin and with higher affinity (Bubb et al., 1994), overnight labeling was necessary to allow FITC-phalloidin to compete with and displace JP. Coverslips were washed three times in 2× PBS for 15 min and inverted on 250 μl of secondary antibody solution (Alexa 546 goat anti-mouse 1:40 in saponin solution) for 1 hr at room temperature. Finally, coverslips were washed three times in 2× PBS for 15 min and mounted onto slides with Slo-fade. Fluorescence signals were detected with a Zeiss LSM410 confocal laser scanning microscope, using a 63x/NA 1.4 objective.

Actin Analysis

DDT_1MF-2 and A7r5 cells were grown under the conditions described above, were scraped and lysed at 4°C in lysis buffer (1% Triton X-100, 20 mM HEPES-NaOH [pH 7.2], 100 mM NaCl, 1 mM sodium orthovanadate, 50 mM NaF, 1 mM PMSF, 1 mM aprotinin, 1 mM leupeptin) and sonicated to disrupt membranes. The lysate was spun at 10,000 g for 20 min. Supernatants contained the detergent-soluble cell fraction (G-actin). Pellets were dissolved in RIPA buffer (15 mM HEPES-NaOH [pH 7.5], 0.15 mM NaCl, 1% Triton X-100, 1% sodium deoxycholate, 0.1% SDS, 10 mM EDTA, 1 mM DTT, 1 mM sodium orthovanadate, 1 mM PMSF, 1 mM aprotinin, 1 mM leupeptin) for 1 hr at 4°C giving the detergent-insoluble fraction (F-actin). Bicinchoninic protein assays were performed on both solutions (G-actin and F-actin) and run on 7% SDS–PAGE gels in equal amounts. Western analysis was performed using a 1:1000 dilution of anti-actin antibody, visualized by chemiluminescence.

Acknowledgments

We greatly thank Paul Luther for assistance in confocal microscopy; Andrjez Janecki for advice on immunostaining; Phillip Crews for generously providing JP and LatA; Mark Donowitz, Carmen Ufret-Vincenty, and Michele Stone for assistance early in the project; Molly-Rose Arnstein for expert graphics; and Sheila Burbidge for inspiration. The work was supported by National Institutes of Health grant HL55426 and a Grant-In-Aid from the American Heart Association, Maryland Affiliate.

Received May 28, 1999; revised July 27, 1999.

References

Alés, E., Tabares, L., Poyato, J.M., Valero, V., Lindau, M., and Alvarez de Toledo, G. (1999). High calcium concentrations shift the mode of exocytosis to the kiss-and-run mechanism. Nat. Cell Biol. *1*, 40–44.

Amieva, M.R., Litman, P., Huang, L., Ichimaru, E., and Furthmayr, H. (1999). Disruption of dynamic cell surface architecture of NIH3T3 fibroblasts by the N-terminal domains of moesin and ezrin: in vivo imaging with GFP fusion proteins. J. Cell Sci. *112*, 111–125.

Becker, K.A., and Hart, N.H. (1999). Reorganization of filamentous actin and myosin-II in zebrafish eggs correlates temporally and spatially with cortical granule exocytosis. J. Cell Sci. *112*, 97–110.

Berridge, M.J. (1995). Capacitative calcium entry. Biochem. J. *312*, 1–11.

Berridge, M.J., Bootman, M.D., and Lipp, P. (1998). Calcium—a life and death signal. Nature *395*, 645–648.

Bird, G.S., and Putney, J.W. (1993). Inhibition of thapsigargin-induced calcium entry by microinjected guanide nucleotide analogues. Evidence for the involvement of a small G-protein in capacitative calcium entry. J. Biol. Chem. *268*, 21486–21488.

Bubb, M.R., Senderowicz, A.M.J., Sausville, E.A., Duncan, K.L.K., and Korn, E.D. (1994). Jasplakinolide, a cytotoxic natural product, induces actin polymerization and competitively inhibits the binding of phalloidin to F-actin. J. Biol. Chem. *269*, 14869–14871.

Carbajal, M.E., and Vitale, M.L. (1997). The cortical actin cytoskeleton of lactotropes as an intracellular target for the control of prolactin secretion. Endocrinology *138*, 5374–5384.

Chen, J., and Mandel, L.J. (1997). Unopposed phosphatase action initiates ezrin dysfunction: a potential mechanism for anoxic injury. Am. J. Physiol. *273*, C710–C716.

Cooper, J.A. (1987). Effects of cytochalasin and phalloidin on actin. J. Cell Biol. *105*, 1473–1478.

Csutora, P., Su, Z., Kim, H.Y., Bugrim, A., Cunningham, K.W., Nuccitelli, R., Keizer, J.E., Hanley, M.R., Blalock, J.E., and Marchase, R.B. (1999). Calcium influx factor is synthesized by yeast and mammalian cells depleted of organellar calcium stores. Proc. Natl. Acad. Sci. USA *96*, 121–126.

Downey, G.P., Takai, A., Zamel, R., Grinstein, S., and Chan, C.K. (1993). Okadaic acid-induced actin assembly in neutrophils: role of protein phosphatases. J. Cell Physiol. *155*, 505–519.

Fasolato, C., Hoth, M., and Penner, R. (1993). A GTP-dependent step in the activation mechanism of capacitative calcium influx. J. Biol. Chem. *268*, 20737–20740.

Favre, B., Turowaski, P., and Hemmings, B.A. (1997). Differential inhibition and posttranslational modification of protein phosphatase

1 and 2A in MCF7 cells treated with calyculin-A, okadaic acid, and tautomycin. J. Biol. Chem. *272*, 13856–13863.

Favre, C.J., Ufret-Vincenty, C.A., Stone, M.R., Ma, H.-T., and Gill, D.L. (1998). Ca^{2+} pool emptying stimulates Ca^{2+} entry activated by *S*-nitrosylation. J. Biol. Chem. *273*, 30855–30858.

Fernando, K.C., Gregory, R.B., Katsis, F., Kemp, B.E., and Barritt, G.J. (1997). Evidence that a low-molecular-mass GTP-binding protein is required for store-activated Ca^{2+} inflow in hepatocytes. Biochem. J. *328*, 463–471.

Ghosh, T.K., Mullaney, J.M., Tarazi, F.I., and Gill, D.L. (1989). GTP-activated communication between distinct inositol 1,4,5-trisphosphate-sensitive and -insensitive calcium pools. Nature *340*, 236–239.

Ghosh, T.K., Bian, J., and Gill, D.L. (1990). Intracellular calcium release mediated by sphingosine derivatives generated in cells. Science *248*, 1653–1656.

Gill, D.L., Ghosh, T.K., Short, A.D., and Waldron, R.T. (1993). GTP-mediated communication between intracellular calcium pools. Handbook Exp. Pharmacol. *108*, 625–649.

Gill, D.L., Waldron, R.T., Rys-Sikora, K.E., Ufret-Vincenty, C.A., Graber, M.N., Favre, C.J., and Alfonso, A. (1996). Calcium pools, calcium entry, and cell growth. Biosci. Rep. *16*, 139–157.

Gregory, R.B., and Barritt, G.J. (1996). Store-activated Ca^{2+} inflow in *Xenopus laevis* oocytes: inhibition by primaquine and evaluation of the role of membrane fusion. Biochem. J. *319*, 755–760.

Holda, J.R., and Blatter, L.A. (1997). Capacitative calcium entry is inhibited in vascular endothelial cells by disruption of cytoskeletal microfilaments. FEBS Lett. *403*, 191–196.

Hosoya, N., Mitsui, M., Futoshi, Y., Ishihara, H., Ozaki, H., Karaki, H., Hartshorne, D.J., and Mohri, H. (1993). Changes in the cytoskeletal structure of smooth muscle cells induced by calyculin-A. J. Cell Sci. *105*, 883–890.

Hoth, M., and Penner, R. (1993). Calcium release-activated calcium current in rat mast cells. J. Physiol. (Lond.) *465*, 359–386.

Irvine, R.F. (1990). "Quantal" Ca^{2+} release and the control of Ca^{2+} entry by inositol phosphates—a possible mechanism. FEBS Lett. *263*, 5–9.

Kerschbaum, H.H., and Cahalan, M.D. (1999). Single-channel recording of a store-operated Ca^{2+} channel in Jurkat T lymphocytes. Science *283*, 836–839.

Kiselyov, K., Xu, X., Mohayeva, G., Kuo, T., Pessah, I.N., Mignery, G.A., Zhu, X., Birnbaumer, L., and Muallem, S. (1998). Functional interaction between $InsP_3$ receptors and store-operated Htrp3 channels. Nature *396*, 478–482.

Kreienbuhl, P., Keller, H., and Niggli, V. (1992). Protein phosphatase inhibitors okadaic acid and calyculin A alter cell shape and F-actin distribution and inhibit stimulus-dependent increases in cytoskeletal actin of human neutrophils. Blood *80*, 2911–2919.

Mackay, D.J., Esch, F., Furthmayr, H., and Hall, A. (1997). Rho- and rac-dependent assembly of focal adhesion complexes and actin filaments in permeabilized fibroblasts: an essential role for ezrin/radixin/moesin proteins. J. Cell Biol. *138*, 927–938.

Matsui, T., Maeda, M., Doi, Y., Yonemura, S., Amano, M., Kaibuchi, K., and Tsukita, S. (1998). Rho-kinase phosphorylates COOH-terminal threonines of ERM proteins and regulates their head-to-tail association. J. Cell Biol. *140*, 647–657.

Matthews, J.B., Smith, J.A., and Hrnjez, B.J. (1997). Effects of F-actin stabilization or disassembly on epithelial Cl^- secretion and Na-K-2Cl cotransport. Am. J. Physiol. *272*, 254–262.

Muallem, S., Kwiatkowska, K., Xu, X., and Yin, H.L. (1995). Actin filament disassembly is a sufficient final trigger for exocytosis in nonexcitable cells. J. Cell Biol. *128*, 589–598.

Neher, E. (1993). Secretion without full fusion. Nature *363*, 497–498.

Parekh, A.B., and Penner, R. (1997). Store depletion and calcium influx. Physiol. Rev. *77*, 901–930.

Petersen, C.C., and Berridge, M.J. (1996). Capacitative calcium entry is colocalised with calcium release in Xenopus oocytes: evidence against a highly diffusible calcium influx factor. Pflugers Arch. *432*, 286–292.

Pietromonico, S.F., Simons, P.C., Altman, A., and Elias, L. (1998). Protein kinase C-q phosphorylation of moesin in the actin binding sequence. J. Biol. Chem. *273*, 7594–7603.

Putney, J.W., and Bird, G.S. (1993). The signal for capacitative calcium entry. Cell *75*, 199–201.

Putney, J.W., and McKay, R.R. (1999). Capacitative calcium entry channels. Bioessays *21*, 38–46.

Randriamanpita, C., and Tsien, R.Y. (1993). Emptying of intracellular Ca^{2+} stores releases a novel small messenger that stimulates Ca^{2+} influx. Nature *364*, 809–813.

Ribeiro, C.M.P., Reece, J., and Putney, J.W. (1997). Role of the cytoskeleton in calcium signaling in NIH 3T3 cells: an intact cytoskeleton is required for agonist-induced $[Ca^{2+}]_i$ signaling, but not for capacitative calcium entry. J. Biol. Chem. *272*, 26555–26561.

Rys-Sikora, K.E., and Gill, D.L. (1998). Fatty acid-mediated calcium sequestration within intracellular calcium pools. J. Biol. Chem. *273*, 32627–32635.

Rys-Sikora, K.E., Ghosh, T.K., and Gill, D.L. (1994). Modification of GTP-activated calcium translocation by fatty acyl-CoA esters: evidence for a GTP-induced prefusion event. J. Biol. Chem. *269*, 31607–31613.

Sakai, T., and Ambudkar, I.S. (1996). Role for protein phosphatase in the regulation of Ca^{2+} influx in parotid gland acinar cells. Am. J. Physiol. *271*, C284–C294.

Shinoki, N., Sakon, M., Kambayashi, J., Ikeda, M., Oiki, E., Okuyama, M., Fujitana, K., Yano, Y., Kawasaki, T., and Monden, M. (1995). Involvement of protein phosphatase-1 in cytoskeletal organization of cultured endothelial cells. J. Cell. Biochem. *59*, 368–375.

Shurety, W., Stewart, N.L., and Stow, J.L. (1998). Fluid-phase markers in the basolateral endocytic pathway accumulate in response to the actin assembly-promoting drug jasplakinolide. Mol. Biol. Cell *9*, 957–975.

Simons, P., Pietromonico, S., Reczek, D., Bretscher, A., and Laurence, E. (1998). C-terminal threonine phosphorylation activates ERM proteins to link the cell's cortical lipid bilayer to the cytoskeleton. Biochem. Biophys. Res. Commun. *253*, 561–565.

Somasundaram, B., Norman, J.C., and Mahaut-Smith, M.P. (1995). Primaquine, an inhibitor of vesicular transport, blocks the calcium-release-activated current in rat megakaryocytes. Biochem. J. *309*, 725–729.

Toivola, D.M., Goldman, R.D., Garrod, D.R., and Eriksson, J.E. (1997). Protein phosphatases maintain the organization and structural interactions of hepatic keratin intermediate filaments. J. Cell Sci. *110*, 23–33.

Trifaro, J.M., Glavinovic, M., and Rose, S.D. (1997). Secretory vesicle pools and rate and kinetics of single vesicle exocytosis in neurosecretory cells. Neurochem. Res. *22*, 831–841.

Tsukita, S., Yonemura, S., and Tsuikita, S. (1997). ERM proteins: head-to-tail regulation of actin-plasma membrane interaction. TIBS *22*, 53–58.

Ufret-Vincenty, C.A., Short, A.D., Alfonso, A., and Gill, D.L. (1995). A novel Ca^{2+} entry mechanism is turned on during growth arrest induced by Ca^{2+} pool depletion. J. Biol. Chem. *270*, 26790–26793.

Yao, Y., Ferrer-Montiel, A.V., Montal, M., and Tsien, R.Y. (1999). Activation of store-operated Ca^{2+} current in *Xenopus* oocytes requires SNAP-25 but not a diffusible messenger. Cell *98*, this issue, 475–485.

Zweifach, A., and Lewis, R.S. (1993). Mitogen-regulated Ca^{2+} current of T lymphocytes is activated by depletion of intracellular Ca^{2+} store. Proc. Natl. Acad. Sci. USA *90*, 6295–6299.